PHYSICAL REVIEW D VOLUME 36, NUMBER 1 1 JULY 1987

Search for fractionally charged particles

R. G. Milner, B. H. Cooper,* K. H. Chang, K. Wilson, J. Labrenz, and R. D. McKeown
W. K. Kellogg Radiation Laboratory, California Institute of Technology, Pasadena, California 91125
(Received 4 September 1986)

An ion source and a charge spectrometer system have been used to search in solid, stable matter for particles with nonintegral charge. Samples of niobium, tungsten, selenium, and meteorites were searched for fractionally charged particles with effective nuclear charge $Z=N+\frac{1}{3}e$ ($N=0,1,\ldots$), and $Z=N+\frac{2}{3}e$ ($N=0,1$). No positive signal was observed and concentration limits are reported.

I. INTRODUCTION

It is generally assumed that quarks and antiquarks of electric charge $\pm\frac{1}{3}e$, $\pm\frac{2}{3}e$ are fundamental constituents of hadrons. Thus it is plausible that free fractionally charged particle (FCP's) might exist in nature, and many experimental searches for such particles have been performed.[1] New interest in searching for FCP's has been generated by reports of the observation of fractional charges on superconducting niobium spheres by LaRue, Phillips, and Fairbank.[2] Their results could indicate the presence of FCP's with electric charge modulo $\frac{1}{3}e$ at a concentration level of at least 2×10^{-18}/Nb atom. It has been pointed out that the fractional charges may be transferred from tungsten during annealing of the niobium sample, and larger concentrations of FCP's may then be expected in tungsten.[3]

Several groups have attempted to perform searches in niobium at the sensitivity indicated by the results of Ref. 2. Some experiments have searched for FCP's under the assumption that the particles will diffuse out of niobium at higher temperatures but will be trapped at lower temperatures.[4] We reported some preliminary results on niobium and tungsten,[5] and an independent niobium levitation experiment was performed by Smith *et al.*[6] All of these efforts yielded negative results with sensitivity exceeding that of Ref. 2.

In addition, several other groups have performed very sensitive searches in other materials, again with negative results.[7] Experiments carried out at San Francisco State University with a modified Millikan oil-drop technique have searched in 4×10^{19} nucleons of refined mercury, 3.4×10^{19} nucleons of water from a variety of natural sources, and samples exposed to heavy-ion collisions at the LBL Bevalac. Both room-temperature diamagnetic and ferromagnetic levitation techniques have been used to set very stringent limits by the Genoa group with, for example, a limit of 1 FCP in 2×10^{21} nucleons established for steel.

In this paper we describe our technique in more detail, and report some new results on niobium, tungsten, selenium, and samples of meteorites. Selenium was chosen because there was a previous measurement in the literature which reported observation of charge $\frac{2}{3}e$ (Ref. 8). The meteorite samples were chosen because they are considered to be some of the oldest material available; some of the meteorites exhibit isotopic abundances which are distinct from those of terrestrial and lunar samples. If free fractional charges did exist during the early stages of the Universe, it is possible that they might still be found among the remnants of the first matter to solidify from the interstellar medium. An upper limit of 10^{-17} FCP per nucleon has already been set[9] for certain samples of meteorites and for FCP's with masses less than 5 GeV/c^2. Our search has covered a wider mass range and has concentrated on samples with isotopic anomalies.

The Semarkona, Murchison CFO_c, and Murchison CFO_fN meteorite samples were obtained from Yang and Epstein of Caltech. A detailed isotopic analysis of each is described in Ref. 10. The Semarkona meteorite contained a component of deuterium-rich organic hydrogen with a D/H ratio more than 80 times higher than the cosmic value of 2×10^{-5}. This suggests that this meteorite contains organic matter that formed before the formation of the solar nebula at temperatures well below 100 K. The other two samples were separates from the Murchison carbonaceous meteorite (CM2 class). The CFO_c sample was a coarse-grained residue from a specified acid-leaching procedure which also contains hydrogen of a high D/H ratio, indicating a similar formation in interstellar clouds. The other separate, CFO_fN, is a fine-grained residue containing unusually high concentrations of ^{13}C-rich carbon. This material is thought to have been produced through nucleosynthesis in red giant stars. The other three samples were obtained from Papanastassiou, also of Caltech. Murchison ME 2642 is a carbonaceous chondrite of the type already discussed. Allende is also a carbonaceous meteorite (CVB class); this meteorite is distinctive because it contains relatively large inclusions, enriched in refractory elements which are considered to be early condensates of the solar nebula. Some of these inclusions contain correlated isotopic anomalies for several elements (e.g., O, Mg, Si, Ca, Ti, Cr, Sr, Ba, Nd, Sm) and also evidence for the *in situ* decay of extinct nuclides. The Colomera is an iron meteorite which contains silicate inclusions which have been dated at 4.6×10^9 yr (Ref. 11). The age of this meteorite is approximately the age of the solar system.

II. GENERAL DESCRIPTION OF EXPERIMENT

The apparatus used in these measurements is shown schematically in Fig. 1. A sputter source atomically decomposes the sample and injects any sputtered ions into a tandem electrostatic accelerator in a mass-independent way. There follows a system of electrostatic analysis which selects particles with a particular electrostatic rigidity (kinetic energy per unit charge). The selected particles are stopped in a detector which measures their kinetic energy. The selection of electrostatic rigidity, combined with the kinetic energy measurement, determines the charge.

The discussion of different charge-states is facilitated by defining the parameter

$$R = \frac{q}{E_K} V_T \ ,$$

where E_K is the kinetic energy, q is the final charge state, and V_T is the tandem terminal potential. Thus, we expect integrally charged ions that strip from charge -1 to charge $+1$, $+2$, $+3$, ... to correspond to R values of $\frac{1}{2}, \frac{2}{3}, \frac{3}{4}, \ldots$. For an FCP, we expect a $-\frac{1}{3}$ ($-\frac{2}{3}$) particle stripped to $+\frac{2}{3}$ ($+\frac{1}{3}$) in the terminal to have an R value of $\frac{2}{3}$ ($\frac{1}{3}$). Of course, the actual R values differ slightly due to the contribution of the source injection energy to the total kinetic energy. The selected charged particle finally comes to rest in a detector which measures its kinetic energy. Hence the charge is determined by a combination of the measured values of R and E_K.

A major concern was that the experiment should be as mass independent as possible, since the mass of the FCP is not known *a priori*. This required that all the optical focusing elements on the beamline be electrostatic and not magnetic.

Another important concern was that the sputter source preferentially select FCP's. It was assumed that the FCP's were present in the sample *ab initio* and the sputtering process caused them to be ejected from the bulk sample to a region where they could be swept away by an electric field. However, this sputtering process also generated secondary ions, which would give rise to a background in the experiment. Thus, a magnetically analyzed 30-keV Ar^+ beam was used to sputter the target in an ultrahigh-vacuum (10^{-9} Torr) environment. This sputtering by a noble gas in a clean vacuum reduced the secondary ion yield.

It was also important to be able to search for both signs of FCP's. Clearly the experiment required negative injection into the tandem accelerator. Thus, for positive charges, electron attachment in a rubidium charge-exchange canal was necessary. Simple chemistry arguments indicate that certain particles will preferentially come off positive and others negative in the sputtering process. In either case our method requires that the FCP be able to bind an electron.

Consider fractionally charged atoms (FCA's) with $Z = N + \frac{1}{3}$ and $Z = N + \frac{2}{3}$, $N = 0, 1, 2, \ldots$. A positively charged FCA present on the sputtering surface will be emitted as a negatively charged object if $A \gtrsim \phi$, where A is the electron affinity and ϕ is the work function. If $A \lesssim \phi$, positive emission is more likely. This simple argument correctly predicts the favored charge states for normal atoms and ions. Lackner and Zweig have investigated the chemistry of fractionally charged atoms[12] and, in particular, have calculated the electronegativity and ionization potential for any such atom in the periodic table. Their results were used as a guide to the chemical properties of FCP's. It is to be noted that by FCP's we include not only quarks but also diquarks, or more exotic objects such as hadronic color singlets, leptons, or even quark constituents.

A direct negative extraction search covers all the $Z = N + \frac{2}{3}$ possibilities, and that region of the $Z = N + \frac{1}{3}$ periodic table[12] where the FCP's will be more likely to come off the surface negatively charged. A positive extraction search followed by charge exchange is sensitive to those regions of the $Z = N + \frac{1}{3}$ table not covered in the direct negative extraction search.

III. EXPERIMENTAL APPARATUS

The method employed involved four steps (see Fig. 1): (a) extraction of the FCP from the host sample and formation of a negative ion; (b) acceleration of negative FCP's and stripping of an electron in a tandem electrostatic accelerator; (c) deflection of the (now positively charged) FCP in a transverse electric field; and (d) measurement of the kinetic energy in a particle detector. Mass independence required both that the magnets at the ion source, terminal, and exit of the tandem accelerator be degaussed to the order of 0.5 g, and that as much as possible of the beamline be shielded with high permeability magnetic shielding. Because the probability for charge-changing collisions in the residual gas of the beamline was proportional to the pressure, it was necessary that the vacuum pressure be $\sim 5 \times 10^{-8}$ Torr.

To extract FCP's from a sample of solid stable matter, a special ion source (see Fig. 2) was designed and built. A sputtering beam of approximately 30 μA of magnetically analyzed 30-keV Ar^+ was focused onto a 1-mm spot on the target in an ultrahigh-vacuum environment. All sputtered ions were collected and accelerated through an initial extraction potential of V_1. This ion yield exhibited a plateau with increasing V_1, indicating 100% collection efficiency. In addition, the aperture diameter in the extractor plate was varied to ensure that no ions were skimmed off at this stage. Bucking coils reduced stray magnetic fields in the extraction region to ≈ 10 mG. An einzel lens focused the extracted particles, which then passed through a 15° electrostatic analyzer. After the analyzer was a rubidium-vapor charge-exchange canal which was used only for positive extraction. Thus the source could be operated in either of two modes. For direct negative extraction the target bias, extractor lens, and 15° electrostatic analyzer are tuned for negative particles. For positive extraction followed by charge exchange, these three elements were tuned for positive particles. The source emittance was calculated to be $\approx 5000\ \pi$ mm mrad $\text{eV}^{1/2}$. Following the charge-exchange canal was an accelerating column with a potential drop of V_2 across it. The total injector bias was given

by the sum of the target bias V_1 and the column bias V_2. These potentials were typically about 8 and 70 kV, respectively. Thus, a negative ion of charge -1 would have energy 78 keV. A directly extracted $-\frac{2}{3}$ particle would have energy 52 keV. A directly extracted $+\frac{1}{3}$ particle which charge exchanged to $-\frac{2}{3}$ would have energy 49.33 keV.

The tandem accelerator used in the experiment was a 3-MV pelletron manufactured by National Electrostatics Corporation. Its voltage stability on generating-voltmeter (GVM) regulation was $\sim 1{:}10^4$. The GVM was calibrated at 496 kV by means of the 992-keV resonance in the $^{27}\mathrm{Al}(p,\gamma)$ reaction. A gas stripper (both H_2 and N_2) pumped by titanium sublimator pumps was used for charge exchange in the terminal. The value of the terminal potential for this experiment was determined by two constraints. The transmission efficiency through the machine improved at lower energies. However, the detector background increased at lower energies so the compromise value of 2 MV was chosen for the $R=\frac{1}{3}$ measurements. The $R=\frac{2}{3}$ search had a 3.4-mg cm^{-2} aluminum detector window and so, to increase the range of the particles, the terminal potential was set to 3 MV. In searching for $Z=\frac{1}{3}$ or $\frac{2}{3}$, maximal stripping of the single bound electron was achieved by using N_2 stripper gas. For other particles, however, the gas used was H_2. This reduced multiple scattering effects and increased the probability for stripping only one of the bound electrons.

The two-stage electrostatic analysis system at the high-energy end was designed to have a resolution of $\sim 0.2\%$ for 2-MeV ions. The first stage was a single set of parallel plates of length 30 cm, gap 3 cm, and produced a deflection of 2.5°. There followed a drift of 1 m to a second stage. This second stage had two sets of parallel plates, each of length 50 cm and gap 3 cm. The total deflection of this second stage was 8°. The plate voltages were balanced so that there was zero potential midway between the plates. When tuned for $R=\frac{1}{3}$, the $R=\frac{1}{2}$, $\frac{2}{3}$, etc., beams did not get past the variable horizontal slit $S2$ (cf. Fig. 1). A fixed slit of width 1.27 cm between the two sets of plates in the second stage of analysis had the function of eliminating any halo which would hit the plates. This slit also put a vertical limitation of 1.90 cm on the beam. To eliminate particles which had scattered from plates in the second stage, a variable slit $S3$ was positioned just after this stage. Further down the beamline there was a fixed collimator of diameter 5 cm to eliminate scattering from the inside of the beam pipe. After the second stage of electrostatic analysis, there followed a drift of length 5.5 m to a 0.5-cm aperture in front of the detector station. This aperture served to define the resolution in electrostatic rigidity. The settings for the object slits $S1$ and horizontal slits $S2$ and $S3$ were obtained using known mass beams from the cesium source, and by demanding that all particles with masses greater than 200 MeV/c^2 be transmitted through the system. The high-energy quadrupoles and electrostatic analysis system were computer controlled, which enabled the easy and precise scaling from one charge state to another.

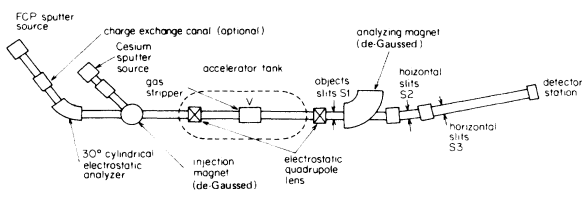

FIG. 1. Schematic diagram of the experimental apparatus.

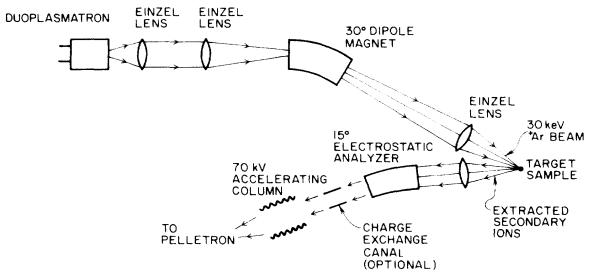

FIG. 2. Schematic diagram of the FCP source.

Because the experiment demanded the detection of heavy ions with MeV energies, it was necessary to calibrate all detectors for pulse-height defect. This calibration agreed with existing prescriptions[13] at the 1–2 % level. We employed two separate detection systems in these measurements. For highly ionizing particles with range less than 20 μm in silicon, a heavy-ion-type Si detector was used. It had an active area of 100 mm^2 and a sensitive depth of ≥ 60 μm at a bias of $+100$ V. It was found that the major source of background in the region of interest, i.e., 0.5–3.0 MeV, was from room γ rays interacting in the depletion region. Thus, the detector was operated at a bias of $+33$ V and surrounded with 5 cm of lead shielding. This resulted in one background count every 4 h in the region from 0.6 to 2.1 MeV.

For lightly ionizing particles a three-stage $E-\Delta E$ detector was used, consisting of a gas detector (GAS), a 500-μm Si detector (Si1), and a 60-μm partially depleted detector (Si2). The gas detector was 30 cm in length and was filled to a pressure of 8 Torr with isobutane. The entrance window to the gas detector was 20 μg cm^{-2} of Formvar, constructed of three layers of equal thickness. The thickness of the window was measured using the 5.486-MeV α line of ^{241}Am. The gas ΔE detector was a gridded ionization chamber. The Frisch grid was constructed from 20-μm gold-plated tungsten wire mounted on a brass frame. The anode was biased at $+300$ V and the grid at $+150$ V. The E detector was mounted in the volume of the gas detector, and was a 500 μm totally depleted Si surface barrier detector. All known stable particles would stop in the GAS or Si1. However, certain types of observable FCP's could penetrate both and to detect these, Si2 was placed after the GAS and Si1 detectors. It was a 60-μm partially depleted silicon detector with an applied bias of $+50$ V. The main source of background in the GAS-Si1-Si2 detector system was the interaction of cosmic rays in the 500-μm-thick depletion region in the Si1 detector. Thus, the gas detector was surrounded on four sides by 0.64-cm-thick plastic scintillator

paddles. The addition of this cosmic veto reduced the cosmic-ray-induced event rate by a factor of 4 to ~ 2 per h.

IV. EXPERIMENTAL METHOD

The first step in the search for FCP's was to establish a set of tuning parameters for mass-independent transmission. Consider the situation for $R = \frac{1}{3}$; i.e., one is looking for FCP's that enter the pelletron with charge $-\frac{2}{3}$ and strip to $+\frac{1}{3}$ in the terminal. The high-energy analyzing magnet was degaussed using a bucking current. Then the cesium source was used to generate beams of hydrogen, oxygen, and copper with identical injection energy to that used with the FCP sputter source. The high-energy analysis system and quadrupoles were tuned for $R = \frac{1}{2}$ (i.e., the $-1 \rightarrow +1$ charge state) and the beams were made spatially coincident at the detector by using magnetic steering elements at the high-energy end of the accelerator. The system was then mass independent for masses between 1 and ~ 65 GeV/c^2 at 4 MeV energy. To ensure this mass independence from 200 MeV/c^2 to ~ 200 GeV/c^2 for 2-MeV particles, the following procedure was used. At each of the three variable slit positions—object, S2, and S3—the positions in space of the hydrogen, oxygen, and copper beams was determined, and the slits were set for an extrapolated lower mass of 200 MeV/c^2.

The cesium source was then shut down, the low-energy inflection magnet degaussed, the argon sputter beam tuned up, and a sputter beam intensity of the order of 30 μA obtained. This beam was then directed onto the desired target and the secondary ion beam was extracted, accelerated, and tuned on the detector station Faraday cup. Only very slight retuning from the cesium source tune was necessary. One of the components of the extracted beam was hydrogen, which provided a check on the mass independence of the system from the sputtering site, where the H^- were formed, to the Si1 detector, where they came to rest. A slight adjustment of the high-energy magnetic steerers was sometimes necessary.

The high-energy quadrupoles and electrostatic analyzer were then scaled from $R = \frac{1}{2}$ $(-1 \rightarrow +1)$ to a background beam of similar rigidity to that of the FCP beam. This background beam resulted from the $+2$ charge state picking up an electron between the end of the accelerating column and the beginning of the analysis system. Finally, one scaled from the $-1 \rightarrow +2 \rightarrow +1$ background beam to the FCP rigidity setting, which involved a rigidity change of only 1.1%.

The mass-independence procedure for the $R = \frac{2}{3}$ search was identical. However, the running procedure was different. Because the $R = \frac{2}{3}$ FCP setting is degenerate with the $+2$ charge state it was necessary to run with 3 MV on terminal and with a 3.4 mg cm^{-2} aluminum foil on the window of the gas detector. This enabled a search for $R = \frac{2}{3}$ particles to be carried out.

The positive extraction search was run at $R = \frac{1}{3}$ with 2 MV on terminal. There were two independent stages of charge-state filtering, and so it was necessary to scale the low-energy optics as well as the high-energy optics. Accordingly, the beam-related background was usually negligible in this search.

Every hour during the search, the data acquisition was halted, to check the beam tuning and ensure that no settings had drifted.

V. EXPERIMENTAL RESULTS

The FCP ion source could be configured to extract either positive or negative particles. When sputtering for the first time on a new niobium target, beam currents as high as 20 nA could be extracted. However, over a period of several hours this current dropped to ~ 2 nA, as surface contaminants were sputtered away. The composition of the direct negative extraction beam was found to be $\sim 80\%$ chlorine, $\sim 15\%$ fluorine, and 5% hydrogen. The niobium targets were made from commercially available niobium obtained from Alfa Products. A sample of the niobium was chemically analyzed and found to contain 2 ppm of chlorine and not more than 0.1 ppm of fluorine. If one assumes 100% ionization, extraction, and collection of the chlorine atoms, then there is excellent agreement between the observed value of 2 nA of beam and the calculated value.

The 2-nA positive extracted beam, when passed through the rubidium charge-exchange canal, produced a negative current exiting the canal. This beam had three main components, which from pulse-height considerations were hydrogen, carbon, and silicon.

Considerable effort was expended in this experiment to ensure that the results be independent of FCP mass, over as large a mass range as possible. The lower-mass limit is affected by two independent considerations: stray magnetic fields and relativistic effects in the high-energy analysis system. The lower-mass limit, due to stray magnetic fields, was conservatively taken to be 200 MeV/c^2. The relativistic effects are important only in the case of $R = \frac{2}{3}$, $Z = \frac{4}{3}$ particles, and in fixing the lower-mass limit at 250 MeV/c^2. The upper-mass limit was taken to be the mass of an uranium nucleus as pulse-height defect effects and stripper performance are uncertain above this mass.

In analyzing the data we assume 100% collection of secondary ions produced by the FCP sputter source. The system was designed to achieve this and there are two independent observations which lend strong support to this assumption. First, the acceptance of the collection system was increased by a factor of 2 with no resulting increase in extracted beam. This was achieved by doubling the size of the extractor hole in the extraction plate. Second, the calculated value of extracted current, based on 100% ionization and extraction of chlorine and fluorine, is in excellent agreement with the observed value.

Consider an argon sputter beam of I μA incident on a target with sputter yield S (sputtered atoms per incident ion). Let the transmission from sputtering site to detector be t. If there are N counts in the FCP window of the detector in T hours, then the FCP concentration C is given by

$$C = 4.4 \times 10^{-17} \frac{N}{T} \frac{1}{SIt} .$$

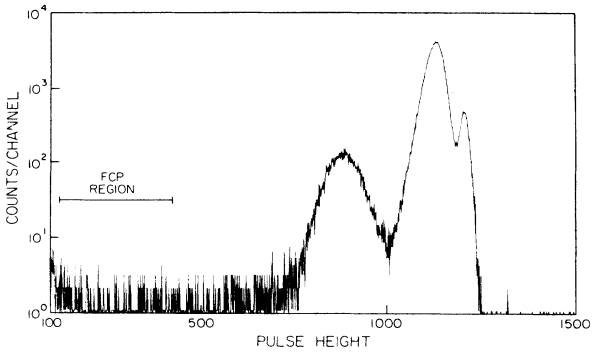

FIG. 3. Energy spectrum for the niobium data for $Z = N + \frac{1}{3}$ particles with electron affinity $\gtrsim 3.5$ eV.

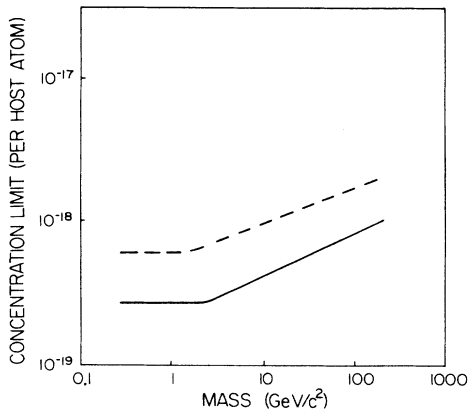

FIG. 5. Improved upper limits for the FCP concentration per target atom in niobium (solid line) and tungsten (dashed line) plotted as a function of FCP mass for $Z = \frac{1}{3}$ particles.

The sputter yield was calculated to be 6.3, 2.5, and 4.6 for niobium, tungsten, and selenium, respectively. This sputter yield was measured for niobium and was in good agreement with the calculated value. Except for the Colomera sample, all meteorites were ground with a mortar and pestle to a very fine powder. To reduce electrostic charging of the meteorite samples, they were mixed with 10-μm copper powder to approximately 50% volume. (This copper also ensured that the temperature in the meteorite powder grains increased $\lesssim 10$ °C.) The ratio by weight of meteorite to copper was measured, as was the total weight of material before and after sputtering. The difference in total material gave the amount of the mixture sputtered. In order to get sputter yields for the meteorite samples themselves, it was assumed that the amount of meteorite sputtered was in the same weight ratio as that of the original mixture. Knowing the total sputtering time for each sample, the rate of meteorite sputtering was calculated. These rates were on the order of 0.4 μg/min.

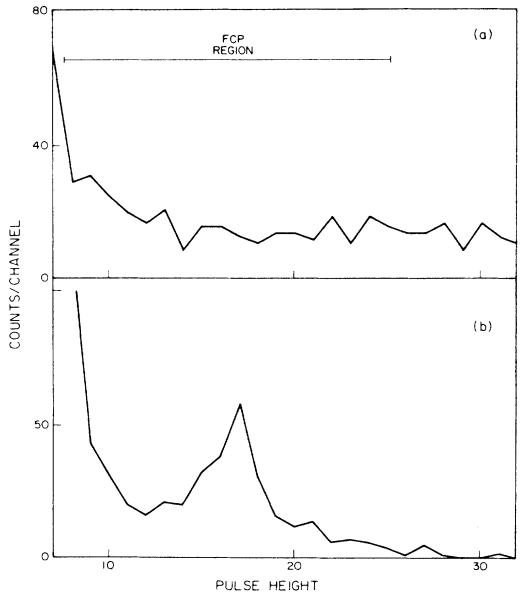

FIG. 4. (a) shows the FCP region of Fig. 3 enlarged. For comparison, (b) shows the 2-MeV Rutherford-scattered peak of niobium ions, scattered through 90° from a 10-μg cm^{-2} gold foil.

The transmission efficiency through the accelerator to the detector was determined as a function of mass with known mass beams from the cesium sputter source. The chlorine beam was used to measure the transmission efficiency for the FCP source. The mass dependence of the transmission efficiency for the FCP source was taken to be that for the cesium source, with the chlorine point providing the normalization factor. For positively-charged-FCP extraction there was an additional transmission factor for ions passing through the charge-exchange canal. This resulted from the velocity dependence of the electron pickup probability in the rubidium vapor and was calculated using the Landau-Zener[14] theory of pseudo-crossing of energy levels. This theory, when applied to integral ions passing through the charge-exchange canal, predicted the transmission efficiency to within 20% of the measured value.

No positive evidence was found for the presence of fractional charges in niobium, tungsten, selenium, or the meteorite samples. Figure 3 shows a typical energy spectrum obtained in a 40-h run on a niobium sample with the FCP source configured in the direct extraction mode

TABLE I. Selenium concentration limits.

Z	Mass (GeV/c^2)	FCP/selenium atom Peak	Integral
$\frac{1}{3}$	$0.2 \lesssim m \lesssim 250$	See Fig. 6(a)	
$\frac{2}{3}$	$0.2 \lesssim m \lesssim 250$	6.5×10^{-15}	
$\frac{5}{3}$	$0.2 \lesssim m \lesssim 4$	6.7×10^{-16}	
$N + \frac{1}{3}$ [a]	$0.7 \lesssim m \lesssim 250$	3.9×10^{-16}	7.2×10^{-15}
$N + \frac{1}{3}$ [b]	$0.7 \lesssim m \lesssim 250$	See Fig. 6(b)	5.7×10^{-17}

[a] $N = 1,2,3,\ldots$ and electron affinity $\gtrsim 4$ eV; negative extraction.
[b] $N = 1,2,3,\ldots$ and electron affinity $\lesssim 4$ eV; positive extraction with rubidium charge exchange.

and the high-energy analysis system tuned for $Z=N+\frac{1}{3}$ particles. The peaks, in order of decreasing pulse height, are due to fluorine, chlorine, and niobium ions which are accelerated as a $+2$ charge state, pick up an electron between the end of the accelerating column and the analysis system, and then are scattered into the detector system. These ions have too high an energy to be FCP's. Figure 4(a) shows the FCP region of Fig. 3 enlarged. For comparison, Fig. 4(b) shows the 2-MeV Rutherford-scattered peak of niobium ions, scattered through 90° from a 10-$\mu g\,cm^{-2}$ gold foil in a calibration run. These data were analyzed to obtain the upper limit of 1.5×10^{-18} for $Z=N+\frac{1}{3}$, $N=1,2,3,\ldots$ FCP's reported in Ref. 5.

In Fig. 5 the improved upper limits for $Z=\frac{1}{3}$ FCP's in niobium (solid line) and tungsten (dashed line) are shown. These resulted from the addition of a thicker Si2 silicon detector in a data run after the results in Ref. 5 were reported. Table I and Fig. 6 summarize the results for selenium. Each line of the table corresponds to different running conditions and particle spectrum analysis. The rise in upper limit at higher masses in Fig. 6 is due to decreasing transmission through the rubidium canal in the case of $Z=\frac{1}{3}$ particles [Fig. 6(a)] and increasing detector background in the case of $Z=N+\frac{1}{3}$ particles [Fig. 6(b)]. The concentration limits obtained for the meteorite samples are summarized in Table II and Figs. 7 and 8. The measured limits differ from sample to sample because of different background rates and running times. The quoted concentration limits are actually estimates since the transmission efficiencies and sputter rates of FCP's are inferred from the behavior of integrally charged ions. In general these estimates are probably accurate to about a factor of 2; however, somewhat larger deviations are conceivable in special cases.

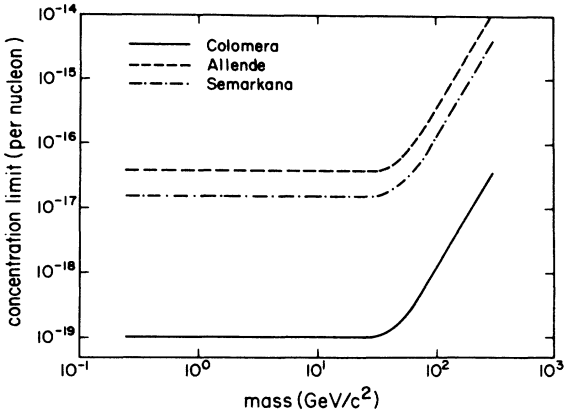

FIG. 7. Upper limits for concentration of $Z=N+\frac{1}{3}$ FCP's in samples of the Colomera, Semarkona, and Allende meteorites.

In summary, we have searched in samples of niobium, tungsten, selenium, and samples of meteorite for fractionally charged particles without a positive signal. The searches for positively charged FCP's are limited by room and cosmic-ray backgrounds, which are reduced in the present experiment by 5 cm of lead shielding and active scintillators, respectively. The searches for negatively charged FCP's are limited by the beam-related background. It is not possible to search for $Z=N+\frac{2}{3}$ ($N=2,3,\ldots$) particles with this technique because of the rigidity degenerate integrally charged background beams. The present results severely constrain the plausible interpretations of the Stanford experiment.[2] In particular, it appears that a heavy-ion-type FCP with $Z=N+\frac{2}{3}$ ($N=2,3,\ldots$) is the only remaining candidate that could be present in appreciable quantities in niobium (i.e., greater than a few FCP's per ball).

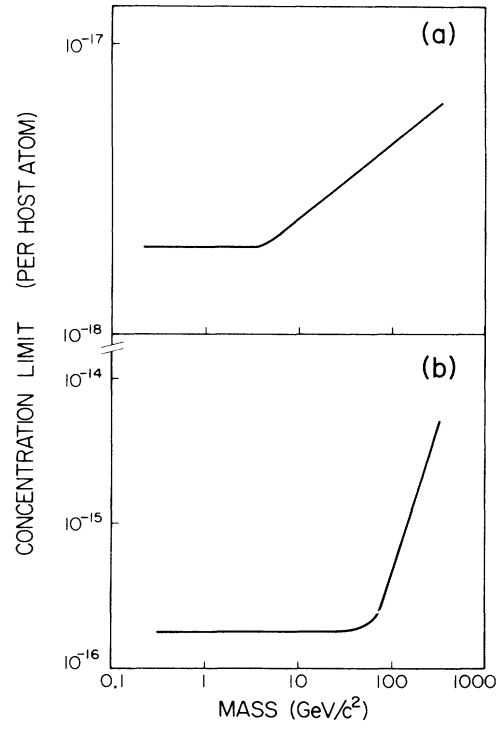

FIG. 6. Upper limit for concentration of FCP's in selenium with (a) $Z=\frac{1}{3}$ and (b) $Z>2$ with low electron affinity.

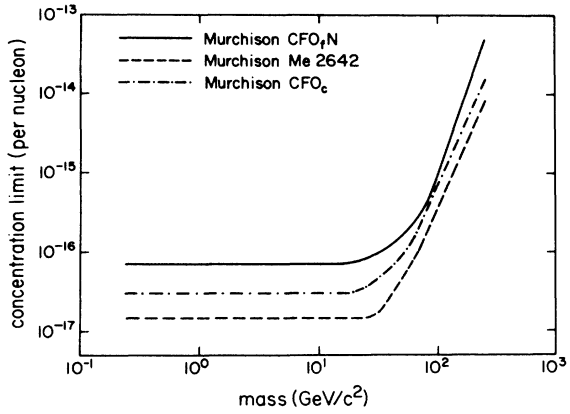

FIG. 8. Upper limits for concentration of $Z=N+\frac{1}{3}$ FCP's in the Murchison samples Me 2642, CFO$_f$N, and CFO$_c$.

TABLE II. Meteorite concentration limits

Z	Mass (GeV/c^2)	Peak concentration (FCP/nucleon) Colomera	Semarkona	Allende	Murchison CFP_c	Murchison CFO_fN	Murchison Me 2642
$\frac{1}{3}$	$0.2 \lesssim m \lesssim 250$	2.7×10^{-19}	3.1×10^{-18}	4.7×10^{-18}	6.7×10^{-18}	1.7×10^{-17}	4.69×10^{-17}
$\frac{2}{3}$	$0.3 \lesssim m \lesssim 250$	2.7×10^{-18}	1.5×10^{-16}	3.6×10^{-17}	4.0×10^{-17}	7.6×10^{-17}	5.2×10^{-17}
$N+\frac{1}{3}$ [a]	$0.2 \lesssim m \lesssim 250$	3.9×10^{-18}	3.9×10^{-18}	9.5×10^{-17}	1.9×10^{-17}	6.6×10^{-16}	4.7×10^{-17}
$N+\frac{1}{3}$ [b]	$0.2 \lesssim m \lesssim 250$	See Fig. 7	See Fig. 7	See Fig. 7	See Fig. 8	See Fig. 8	See Fig. 8

[a] $N = 1,2,3,\ldots$ and electron affinity $\gtrsim 3.5$ eV; negative extraction.
[b] $N = 1,2,3,\ldots$ and electron affinity $\lesssim 3.5$ eV; positive extraction.

ACKNOWLEDGMENTS

We would like to thank Dr. George Zweig for his support and advice throughout this experiment, and for providing us with the selenium samples. We acknowledge Mr. Wilfred Schick for his engineering and mechanical expertise in constructing most of the apparatus. We would also like to thank Dr. D. Papanastassiou, Dr. J. Yang, and Professor S. Epstein for providing us with the meteorite samples. This research was supported by the National Science Foundation under Grants Nos. PHY82-15500 and PHY85-05682 and by the California Institute of Technology Sloan Fund.

*Present address: Physics Department, Cornell University, Ithaca, NY 14853.

[1] L. W. Jones, Rev. Mod. Phys. **49**, 717 (1977).
[2] G. S. LaRue, J. D. Phillips, and W. M. Fairbank, Phys. Rev. Lett. **46**, 967 (1981).
[3] J. D. Morgan III and M. V. Barnhill III, Phys. Rev. Lett. **133B**, 227 (1983).
[4] J. P. Schiffer *et al.*, Phys. Rev. D **17**, 2241 (1978); W. Kutschera *et al.*, *ibid.* **29**, 791 (1984).
[5] R. G. Milner *et al.*, Phys. Rev. Lett. **54**, 1472 (1985).
[6] P. F. Smith *et al.*, Phys. Lett. **153B**, 188 (1985).
[7] C. L. Hodges *et al.*, Phys. Rev. Lett. **47**, 1651 (1981); D. C. Joyce *et al.*, *ibid.* **51**, 731 (1983); M. A. Lindgren *et al.*, *ibid.* **51**, 1621 (1983); W. Marinelli and G. Morpurgo, Phys. Rep. **85**, 161 (1982).
[8] F. E. Ehrenhaft, Phys. Z. **39**, 673 (1938).
[9] W. A. Chupka, J. P. Schiffer, and C. M. Stevens, Phys. Rev. Lett. **17**, 60 (1966).
[10] J. Yang and S. Epstein, Nature (London) **311**, 544 (1984).
[11] H. G. Sanz, D. S. Burnett, and G. J. Wasserburg, Geochim. Cosmochim. Acta **34**, 1227 (1970).
[12] K. S. Lackner and G. Zweig, Phys. Rev. D **28**, 28 (1983).
[13] S. B. Kaufman *et al.*, Nucl. Instrum. Methods **115**, 47 (1974).
[14] J. B. Hasted, Adv. Electron. Electron Phys. **13**, 1 (1960).